Comptes rendus - Geoscience 351 (2019) 312–320

Contents lists available at ScienceDirect

Comptes rendus - Geoscience

www.journals.elsevier.com/comptes-rendus-geoscience

Petrology, Geochemistry (Ore Deposits)

# The ore genesis of the Jebel Mecella and Sidi Taya F–Ba (Zn–Pb) Mississippi Valley-type deposits, Fluorite Zaghouan Province, NE Tunisia, in relation to Alpine orogeny: Constraints from geological, sulfur, and lead isotope studies

Nejib Jemmali [a, *], Larbi Rddad [b], Fouad Souissi [c], Emmanuel John M. Carranza [d, e, f]

[a] Faculté des sciences de Gafsa, Sidi Ahmed Zarrouk, 2112 Gafsa, Tunisia
[b] Earth and Planetary Division, Department of Physical Sciences, Kingsborough Community College of the City University of New York, 2001 Oriental Boulevard, Brooklyn, NY 11235-2398, USA
[c] Université de Tunis El Manar, Faculté des sciences, Département de géologie, 2092 El Manar, Tunis, Tunisia
[d] Economic Geology Research Centre (EGRU), James Cook University, Townsville, Queensland, Australia
[e] Geological Sciences, School of Agricultural, Earth and Environmental Sciences, University of KwaZulu-Natal, South Africa
[f] Institute of Geosciences, State University of Campinas, Campinas, São Paulo, Brazil

ARTICLE INFO

*Article history:*
Received 26 September 2018
Accepted 15 November 2018
Available online 20 March 2019
Handled by François Chabaux

*Keywords:*
F–Ba (Zn–Pb)
Fluorite Zaghouan province
Jebel Mecella
Sidi Taya
S isotope
Pb isotope
MVT

ABSTRACT

Jebel Mecella and Sidi Taya F–(Ba–Pb–Zn) deposits are located within the Fluorite Zaghouan Province (NE Tunisia). The mineralization occurs along the unconformity surface between the Jurassic limestones and Upper Cretaceous rocks. The mineralization consists mainly of fluorite, barite, sphalerite, and galena. The $\delta^{34}S$ values of barite at Jebel Mecella (14.8–15.4‰) and at Sidi Taya (21.6–22.2‰) closely match those of the Triassic evaporites and Messinian seawater, respectively. The range of $\delta^{34}S$ values of galena and sphalerite in both deposits (−6.9 to +2.4‰) suggests the involvement of thermochemical sulfate reduction and possibly organically-bound sulfur in the generation of sulfur. Lead isotope data with $^{206}Pb/^{204}Pb$, $^{207}Pb/^{204}Pb$, and $^{208}Pb/^{204}Pb$ ratios of 18.893–18.903, 15.684–15.699, and 38.850–38.880, respectively suggests a single homogeneous source reservoir of Paleozoic age and/or the homogenization of the Paleozoic–Cretaceous multireservoir-derived fluids along their long migration paths to the loci of deposition during the Alpine orogeny.



## 1. Introduction

The Fluorine Zaghouan Province F–Ba–Sr (Zn–Pb) deposits (FZP) are located in the northeastern part of Tunisia. The mineralization of Jebel Mecella and Sidi Taya, focus of this study, is hosted in the Kimmeridgian–Tithonic–Berriasian "Ressas Formation" (Souissi et al., 1997, 2013; Touhami, 1979). These deposits preferentially occur along or near the NE–SW-trending lineament Zaghouan deep thrust fault. Mineralization occurs as stratabound bodies, karstic and veins in silicified limestones and marls. Based on fluid inclusions studies carried out on fluorite, Souissi et al. (1997) proposed that fluorites and quartz in the FZP were deposited from moderate to high saline hydrothermal mineralizing fluids (e.g., Jebel Stah, Sidi Taya, Hammam Zriba). With regards to sulfur and metal sources, Jemmali et al. (2017) and Souissi et al. (2013) investigated the Jebel Ressas and Hammam Zriba ore deposits and

* Corresponding author. Department of Geology, Faculty of Sciences of Gafsa, Sidi Ahmed Zarrouk, 2112, Gafsa, Tunisia.
*E-mail address:* nejib.jemmali@yahoo.fr (N. Jemmali).

https://doi.org/10.1016/j.crte.2018.11.006
1631-0713/

suggested that Triassic evaporites are the main source of sulfur for sulfides and sulfates and the upper Paleozoic deep parts of the basin as the source of metals. While some FZP ore deposits were investigated previously, the ore genesis of others, however, is not thoroughly studied. The Jebel Mecella and Sidi Taya ore deposits are among these deposits where the sources of sulfur and metals, the mechanisms of ore-forming fluid transport and ore precipitation, and the age of ore emplacement remain poorly constrained. Moreover, researchers focused on the nature of the ore-forming fluids and little attention was given to the source of sulfur and metals for sulfides and sulfates in the studied ore deposits. The present study attempted to fill this gap by reporting and interpreting the results of comprehensive sulfur and lead isotopes data of both Jebel Mecella, and Sidi Taya deposits. The integration of these isotopic data with available geological and geochemical data from the literature allowed the authors to constrain the source(s) of sulfur and metals of the ore. By constraining the source(s) of sulfur and metals, a comprehensive ore genetic model can be established for these ore deposits.

## 2. Geology and ore distribution

The Jebel Mecella and Sidi Taya F–Ba (Zn–Pb) deposits are located along the NE–SW-trending Zaghouan thrust Fault (Fig. 1). The stratigraphy of these deposits is characterized by sedimentary series ranging from the Triassic to the Pliocene–Quaternary (Souissi, 1987; Touhami, 1979; Turki, 1985) (Figs. 2 and 3).

- Triassic rock series: the lithology of the Triassic series is relatively heterogeneous and consists of breccias of gypsum, which outcrop only at Jebel Mecella, variegated clays, sandstones, and black bituminous dolostones.
- Upper Jurassic rock series (Ressas Formation): these series consist of massive bioclastic gray micritic limestones. Their thickness varies from 120 m to 300 m at Jebel Mecella and Sidi Taya, respectively. The mineralization hosted by these series consists of fluorite, barite and minor galena and sphalerite.
- Cretaceous rock series, which consist of:
  - Berriasian rocks (2–10 m), consisting of siliceous bioclastic black limestones overlying in discontinuity the upper Jurassic Ressas Formation;
  - Valanginian–Hauterivian (Neocomian) rocks (100–140 m), which are clayey-limestones and marls intercalations. This level constitutes the hanging wall of the mineralization;
  - the Barremian rocks (170 m) is represented by dark marls with intercalations of clayey limestones and rare beds of quartzite, which outcrop only in the NW flank of the Jebel Mecella.
- Albian-Cenomanian rocks (100–300 m): at the northwestern flank of Jebel Mecella are outcrops of alternating facies of the Albian–Vraconian marl–limestone (Fahdene Formation).
- The Eocene–Oligocene and Miocene rocks (up to 200 m): outcrops are visible only at Sidi Taya and consist of marls with rare intercalations of marl-limestones.
- The Pliocene–Quaternary consists of continental sedimentary series, mainly conglomerates and sandy clays.

The Zaghouan ore district is part of a complex Mesozoic–Tertiary tectonic evolution that affected northeastern Tunisia. This district was affected by two major compressional events, which are the first and second Alpine compressional phases of Eocene and Upper Miocene age, respectively. These compressional phases overlapped with extensional events that occurred in the Oligocene, early–middle Miocene and Pliocene–Early Quaternary (Arfaoui et al., 2017; Ben Ayed, 1993; Bouaziz et al., 2002). The studied ore deposits were affected by most of these tectonic events. With regards to the tectonic setting at Sidi Taya (Souissi, 1987), the limestones of Ressas Formation constitute a monocline structure, dipping 40°–55° NNE. This structure was affected by a vertical NE–SW-trending major fault called Zaghouan Fault. The reactivation of this fault during the Alpine orogeny resulted in the uplift of the limestones (Turki, 1985). This brittle tectonic had also fractured the limestone of the Ressas Formation and resulted in the brecciation of the Lower Cretaceous marl limestones. Field observation of this brittle tectonics at Sidi Taya led to distinguish three different fault systems (Souissi, 1987, Fig. 3). The first fault system that crosscuts the Ressas Formation consists of N100–N120°E-trending normal faults, dipping 30°–40° NNE. These faults are mineralized and were formed during the Cretaceous extensional phase. The second system truncated the previous N100–N120°E-trending normal faults and consists of major NE–SW-trending faults, which include the Zaghouan thrust Fault. These faults also host the mineralization and occurred and were reactivated during the upper Miocene phase. The third fault system, formed during the Pliocene–Early Quaternary extensional phase, is represented by N110–N120°E– and N160–N170°E-trending vertical to sub-vertical, normal faults, which are usually filled with calcite and crosscut both the Ressas Formation and the Jurassic–Cretaceous breccias. According to Touhami (1979), Jebel Mecella is an asymmetric anticline, with a Jurassic core with horst and graben structures on the western flank. These structures are delimited by NW–SE-trending normal faults, which facilitated the upward migration of mineralizing fluids to the paleo-surface (Fig. 2). Owing to the proximity of the NE–SW Zaghouan thrust fault, the hinge of the anticline structure, which consists mainly of Jurassic limestone, was intensively deformed and brecciated. Based on the crosscutting relationship among the three fault sets described above, the chronological order, from the oldest to the youngest, of the development of these faults is established as follows: (i) N100–N120°E-trending normal faults; (ii) NE–SW-trending faults; and (iii) N110–N170°E -trending faults. These three sets of faults were reactivated during the Alpine orogeny and acted as potential pathways for the ore-forming fluids (Souissi et al., 1997).

## 3. Mineralization

The distribution of ore at Jebel Mecella is controlled by the unconformity surface between a footwall of the Ressas

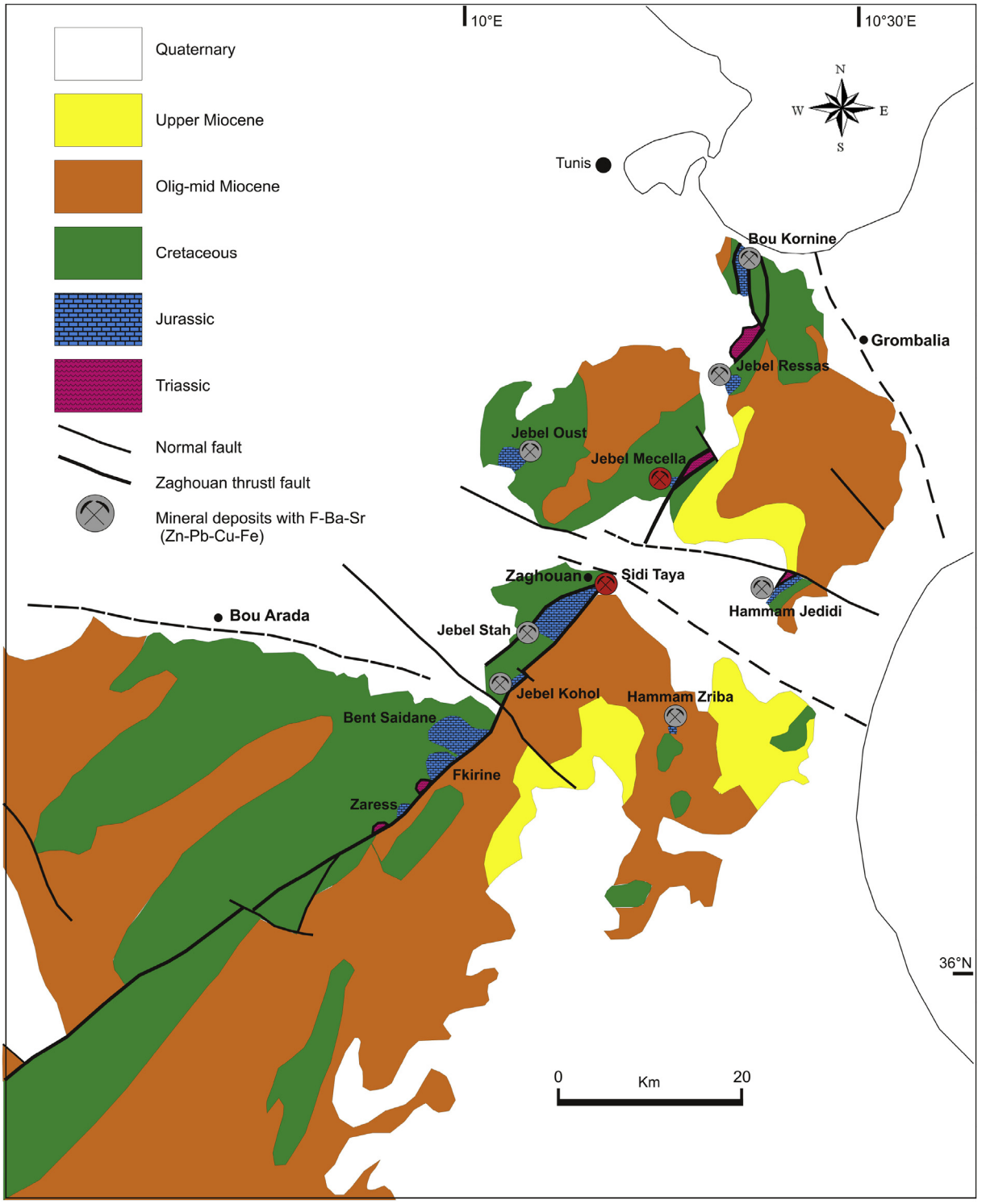


**Fig. 1.** Tectonic and metallogenic map of the Fluorite Zaghouan Province (modified from Morgan et al., 1998) showing the approximate locations of the Jebel Mecella and Sidi Taya deposits.

Formation's carbonates and a hanging wall of the Valanginian–Hauterivian marls (Fig. 2). The ore is also tectonically controlled. In fact, the Jebel Mecella deposit is located near an important structural NE–SW-trending lineament that corresponds to the Zaghouan thrust Fault. According to Touhami (1979), mineralization at Jebel Mecella occurs as (i) lenticular orebodies along the Jurassic–Cretaceous unconformity; and (ii) karstic

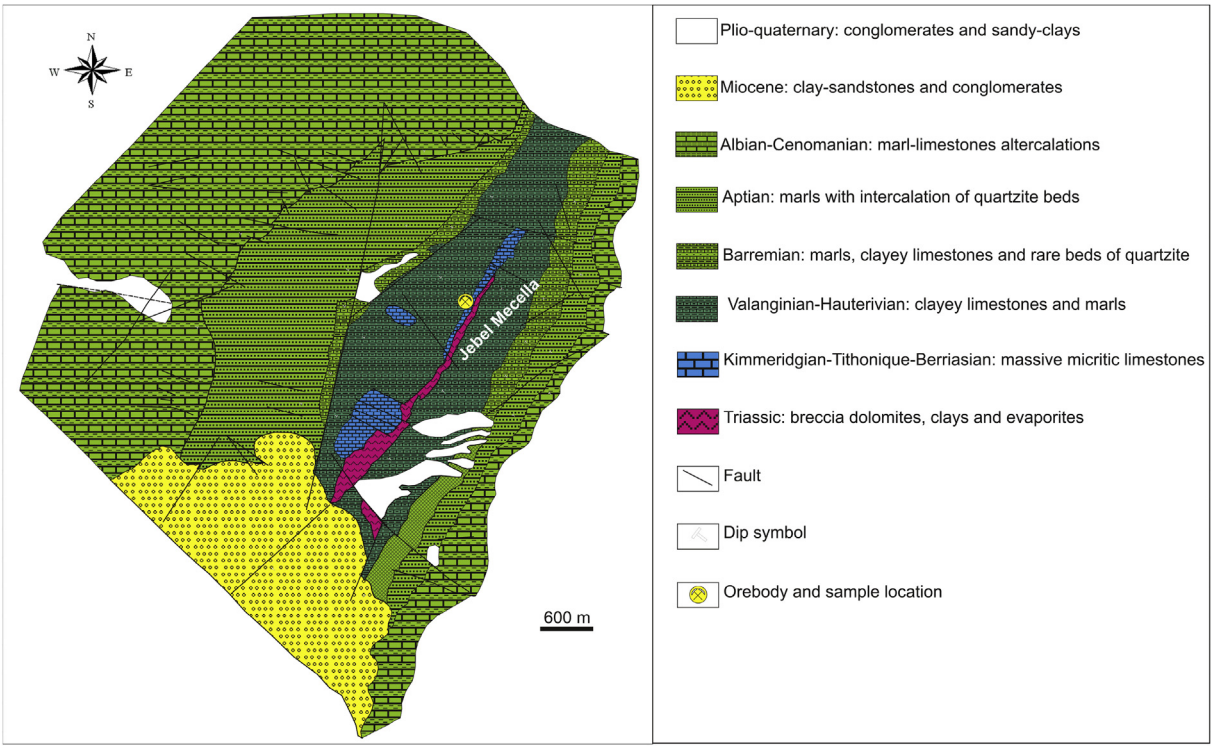


**Fig. 2.** Geological map of Jebel Mecella (modified from Touhami, 1979).

orebodies within the carbonate Ressas Formation. In the lenticular orebodies, fluorite occurs as 5–20-cm-thick bands of white to translucent crystals. These bands alternate with bands of organic matter-rich black siliceous bituminous carbonates with occurrences of honey-colored translucent sphalerite crystals and rare spherulites of barite and celestite; the latter mineral forms the cement of fluorine crystals. In the karstic orebodies, sulfide- and sulfate-rich ore in the Ressas Formation are hosted within densely fractured networks located near the hanging wall contact. Sulfide fillings are hosted in brecciated and fractured limestone and are mainly represented by massive galena and rare sphalerite crystals. These sulfides are cemented by barite-celestite that occur as powdery or needle-like shape. Disseminated pyrite crystals occur in limestone as well as inclusions within sphalerite, and fluorite. Calcite occurs as white crystals within the karst and the host limestones. At Sidi Taya, two main ore styles are recognized (Souissi, 1987): (i) disseminated and (ii) karstic. Disseminated ores consist of mm-to cm-sized crystals of sphalerite and galena with subordinate tetrahedrite, celestite, and barite. These minerals are disseminated within the Upper Jurassic (Kimmeridgian–Tithonic–Berriasian) limestone, which is rich in bipyramidal quartz crystals. Galena and sphalerite occur as mm-to cm-sized euhedral crystals and are mainly associated with organic matter-rich black siliceous limestones, and occasionally with fibrous barite and celestite. The karstic ore style is hosted within the Jurassic limestones associated with E–W-trending fractures. Fluorite occurs as massive, colorless, euhedral crystals and is associated with galena and subordinate sphalerite with traces of tennantite, pyrite, and chalcopyrite, barium-strontium sulfates, and quartz. Galena and sphalerite represent 1–10% of karstic filling and occur both as mm-to cm-sized crystals. The ore mineralogy of both ore deposits is similar and consists of at least four mineralizing stages (Bejaoui, 2012; Souissi, 1987; Touhami, 1979; this work). An early stage is represented by the silicification of the carbonates of the Ressas Formation. This silicification consists of mm-to cm-sized euhedral quartz. The second and main stage consists of galena, sphalerite, and pyrite. The third stage is composed of barite-celestite and fluorite. The last stage is represented by calcite.

## 4. Sampling and methods

A total of 30 ore samples (sulfides and sulfates) from the Jebel Mecella and Sidi Taya F–Ba (Zn–Pb) deposits, especially from lenticular and karstic orebodies, were taken from the unconformity zone between a footwall sequence of predominantly bioclastic limestones of the Ressas Formation and a hanging wall of marls attributed to the Valanginian. Selected samples were subjected to electron probe microanalysis (EPMA) for trace elements in assessment of pyrite and sphalerite. The EPMA was carried out at the Earth Science Department, State University of Milan, Italy, using a JEOL JXA-8200 electron probe equipped with five wavelength-dispersive spectrometers. Sulfur isotope compositions of galena ($n = 16$), sphalerite ($n = 6$) barite ($n = 8$), and gypsum ($n = 2$) were acquired at the Institute of Mineralogy and Geochemistry of the University of

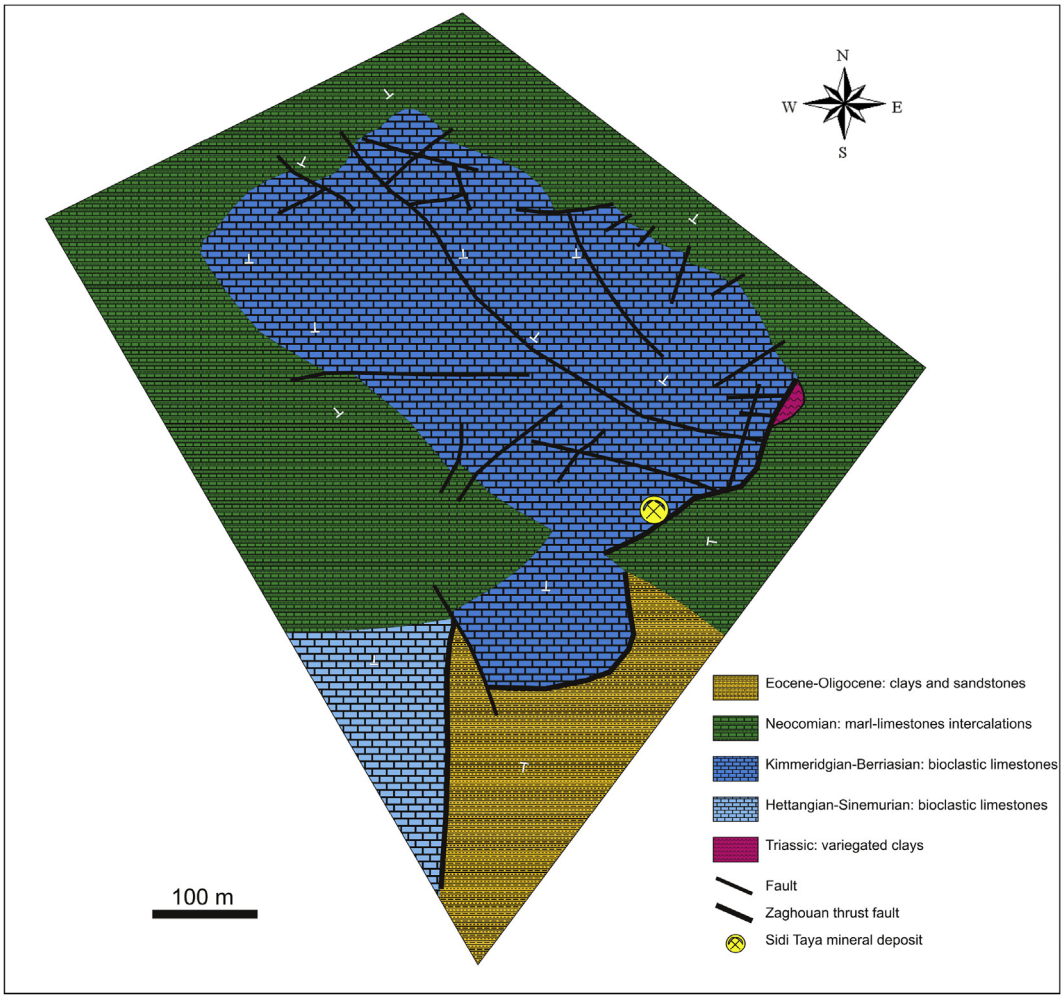


**Fig. 3.** Geological map of Sidi Taya (modified from Souissi, 1987).

Lausanne (Switzerland) using a Carlo Erba 1100 elemental analyzer (EA) connected to a Thermo Fisher Delta S isotope ratio mass spectrometer (IRMS). Lead isotope compositions were measured on galena from selected ore samples ($n = 23$). Pb isotope compositions were analyzed using a multicollector-inductively coupled plasma mass spectrometer (MC-ICP-MS) instrument (Nu Instruments Ltd) at the Radiogenic Isotope facility at the University of Bern (Switzerland).

## 5. Results

### 5.1. Sulfur isotopic composition

In order to constrain the source(s) of sulfur present in sulfides and sulfates, barite samples ($n = 8$) were collected from ore deposits from the karst of Sidi Taya and Jebel Mecella, whereas sulfides (sphalerite and galena) were sampled from lenticular and karst of both deposits. Sulfur isotope values of barites from Jebel Mecella (Table 1, Fig. 4) exhibit a narrow range of 14.8–15.4‰. These values plot within the range of those of the Triassic evaporites outcropping at Jebel Ressas (Fig. 4; Jemmali, 2011). In contrast, barites from Sidi Taya have heavy $\delta^{34}S$ values ranging from 21.6 to 22.2‰. This isotopic composition overlaps with the signature of the Messinian seawater (20.7–24‰; Claypool et al., 1980). The overall $\delta^{34}S$ values of sulfides from Jebel Mecella deposit range from −4.3 to −5.9‰ and from −2.2 to −2.9‰ for galena and sphalerite, respectively (Table 1, Fig. 5). Galena samples of the Sidi Taya also display a narrow range of $\delta^{34}S$ values varying between −6.9 and + 2.4‰ (Table 2, Fig. 5).

### 5.2. Lead isotopic composition

Twenty-three samples of galena, from different orebodies, were analyzed for Pb isotopic compositions to shed light on the possible source(s) of lead and by inference other metals. The Pb-isotope data are presented in Table 2 and plotted on conventional co-variation uranogenic and thorogenic diagrams in Fig. 6. Other ore deposits in the Fluorine Zaghouan Province were also plotted in these diagrams for comparison. The Pb isotope ratios of galena samples of Jebel Mecella deposit are homogeneous

($^{206}Pb/^{204}Pb$ = 18.891–18.903; $^{207}Pb/^{204}Pb$ = 15.684–15.699, and $^{208}Pb/^{204}Pb$ = 38.850–38.880). The Pb isotope ratios of galena samples from the Sidi Taya deposit are also homogenous, ranging from 18.945 to 18.955 for $^{206}Pb/^{204}Pb$, 15.688 to 15.699 for $^{207}Pb/^{204}Pb$, and 38.845 to 38.883 for $^{208}Pb/^{204}Pb$.

## 6. Discussion

### 6.1. Source(s) of sulfur and precipitation mechanisms

The sulfur isotopic composition of barites from Jebel Mecella ($\delta^{34}S$ values = 14.8–15.4‰) falls within the range of those of the Jebel Ressas's Triassic evaporites (15–17.9‰) and Triassic seawater (11–20‰; Claypool et al., 1980). Therefore, it can be suggested that Triassic evaporites are the main source of sulfur in barite from the Jebel Mecella. This is consistent with the occurrence of abundant Triassic evaporitic series outcropping in the proximity of the Jebel Mecella ore deposit. The proposed source of sulfur was also reported by numerous researchers for the majority of the Pb–Zn deposits in Tunisia (e.g., Charef, 1986; Decrée et al., 2008; Jemmali, 2011; Souissi et al., 2013). Conversely, the $\delta^{34}S$ values of the Sidi Taya deposits (21.6–22.2‰) is consistent with the range observed for the Messinian seawater (20.7–24‰; Claypool et al., 1980) and are closer to those of the Triassic evaporites. It can be suggested that the sulfur of this ore derived from the dissolved sulfates of the Triassic evaporites and the Messinian seawater. The latter

**Table 1**
Sulfur isotope data from Jebel Mecella and Sidi Taya sulfides and sulfates.

| Name of the deposit | Mineral phase | $\delta^{34}S$ (‰, VCDT) |
|---|---|---|
| Jebel Mecella | Karstic galena | −5.7 |
| | | −5.9 |
| | | −5.6 |
| | | −4.6 |
| | | −4.7 |
| | | −4.3 |
| | Karstic sphalerite | −2.5 |
| | | −2.2 |
| | | −2.4 |
| | | −2.5 |
| | Lenticular sphalerite | −2.9 |
| | | −2.8 |
| | Karstic barite | 14.8 |
| | | 15.3 |
| | | 15.0 |
| | | 15.4 |
| | Gypsum | 15.2 |
| | | 16.0 |
| Sidi Taya | Disseminated galena | 2.4 |
| | | 2.3 |
| | Karstic galena | −6.9 |
| | | −6.9 |
| | | −5.0 |
| | | −4.9 |
| | | −6.2 |
| | | −6.1 |
| | | −3.8 |
| | | −3.7 |
| | | 21.8 |
| | Karstic barite | 21.6 |
| | | 22.2 |
| | | 22.0 |

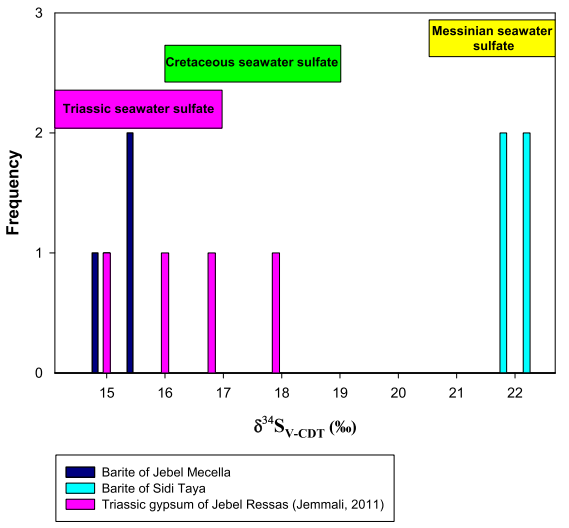


**Fig. 4.** Sulfur isotope compositions of sulfates (barite) from the Jebel Mecella and Sidi Taya deposits and $\delta^{34}S$ ranges for Triassic gypsum from the Jebel Ressas deposit (Jemmali, 2011). Also shown for comparison is the sulfur isotope range for Triassic and Messinian seawater sulfate (Claypool et al., 1980).

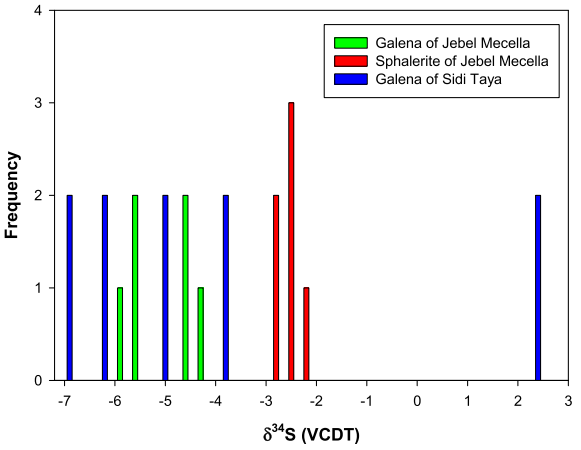


**Fig. 5.** Sulfur isotope compositions of sulfides (galena and sphalerite) from the Jebel Mecella and Sidi Taya deposits.

was also proposed as a source for the Sidi Driss deposit located in northern Tunisia (Decrée et al., 2008). The sulfur isotope compositions of galena from both deposits have $\delta^{34}S$ values ranging from −6.9 to +2.4‰ (avg. of −5.9‰ for Jebel Mecella; avg. of −3.9‰ for Sidi Taya.) The $\delta^{34}S$ values of sphalerite from Sidi Taya vary between −2.2 and −2.9‰ (avg. of −2.5‰). Possible mechanisms explaining sulfur reduction from sulfate include bacterial sulfate reduction (BSR) and thermochemical sulfate reduction (TSR). These processes are temperature-dependent. BSR typically occurs under relatively low temperatures (less than 60–80 °C; Machel, 2001). TSR takes place at a temperature environment fluctuating mainly between 80 and 130 °C (Orr, 1974). This temperature range generally does not sustain microbial life (Machel, 2001). Sulfur isotope compositions of

**Table 2**
Lead isotope data from Jebel Mecella and Sidi Taya.

| Name of the deposit | $^{206}Pb/^{204}Pb$ | $^{207}Pb/^{204}Pb$ | $^{208}Pb/^{204}Pb$ |
|---|---|---|---|
| Mecella | 18.903 | 15.695 | 38.861 |
| | 18.901 | 15.695 | 38.856 |
| | 18.895 | 15.684 | 38.852 |
| | 18.902 | 15.699 | 38.880 |
| | 18.895 | 15.689 | 38.854 |
| | 18.891 | 15.687 | 38.850 |
| | 18.898 | 15.692 | 38.857 |
| Sidi Taya | 18.945 | 15.692 | 38.863 |
| | 18.952 | 15.699 | 38.883 |
| | 18.948 | 15.695 | 38.872 |
| | 18.954 | 15.698 | 38.879 |
| | 18.952 | 15.697 | 38.876 |
| | 18.953 | 15.697 | 38.877 |
| | 18.951 | 15.697 | 38.867 |
| | 18.941 | 15.688 | 38.845 |
| | 18.945 | 15.692 | 38.855 |
| | 18.947 | 15.694 | 38.863 |
| | 18.945 | 15.692 | 38.857 |
| | 18.947 | 15.694 | 38.869 |
| | 18.955 | 15.699 | 38.876 |
| | 18.952 | 15.696 | 38.873 |
| | 18.946 | 15.690 | 38.870 |
| | 18.951 | 15.696 | 38.873 |

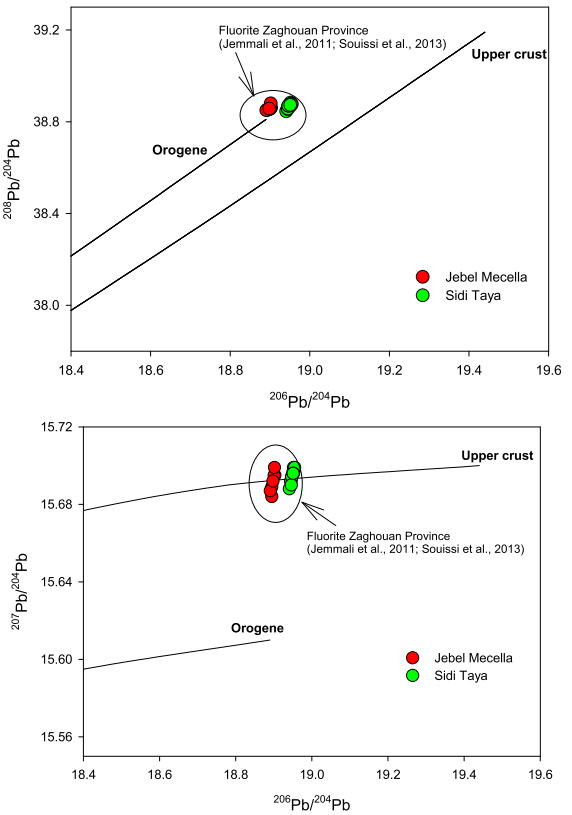


**Fig. 6.** Plots of $^{207}Pb/^{204}Pb$ vs. $^{206}Pb/^{204}Pb$ and $^{208}Pb/^{204}Pb$ vs. $^{206}Pb/^{204}Pb$ for the Jebel Mecella and Sidi Taya deposits (this study), Fluorite Zaghouan Province (Jemmali et al., 2011a; Souissi et al., 2013). Curves of growth trends for Pb isotope ratios are from the plumbotectonic model of Zartman and Doe (1981).

sulfides generated through BSR are by around 40‰ lower than those of the original sulfates (Ohmoto and Rye, 1979). However, fractionation induced by TSR of sulfate to sulfide can lower $\delta^{34}S$ to values around 15‰ lighter than those of the parent sulfates in MVT hydrothermal systems (e.g., Orr, 1974; Ohmoto et al., 1990). The difference between $\delta^{34}S_{SO_4}$ and $\delta^{34}S_{H_2S}$ is approximately 14–24‰ (Krouse et al., 1988). The homogenization temperatures of the fluid inclusions at Jebel Mecella range from 145 to 170 °C for fluorite (Souissi, 1987) and from 129 to 145 °C for sphalerite (Bejaoui, 2012). Homogenization temperatures in the fluorite from Sidi Taya range from 135 to 150 °C (Souissi et al., 1997). These high ore-forming temperatures are not favorable for bacterial activity, and, thus, in situ BSR is a priori excluded as a mechanism for sulfate reduction. It follows that the TSR of dissolved sulfates of the Triassic evaporites and Messinian seawater is considered the main reducing process that generated enough sulfur for the formation of the ore. This is consistent with the calculated fractionation difference between sulfates and sulfides ($\delta^{34}S_{SO_4} - \delta^{34}S_{H_2S} = 17–25‰$). Moreover, TSR mechanism is supported by the presence of sufficient $SO_4^{2-}$ anions provided by pervasive evaporites and reactants such as organic bituminous dolostones and hydrocarbons (Souissi, 1987). In the studied ore deposits, the absence of sphalerite with microspherulitic or colloform textures typical of BSR described in several ore deposits (e.g., Hazelhurst salt dome, Mississippi, Southam and Saunders, 2005; the Bleiberg Zn–Pb deposit, the Sidi Driss and Douahira Pb–Zn deposits, northern Tunisia; Decrée et al., 2008) also points to TSR. Furthermore, no galena with BSR-related skeletal or framboidal textures described by Fallick et al. (2001) in Navan, Ireland, was observed in the Mecella–Sidi Taya ore deposits. The observed negative $\delta^{34}S$ values in sulfides of the Mecella–Sidi Taya ore deposits can be, therefore, explained by (i) BSR mechanism that may have taken place prior to the onset of the hydrothermal ore-forming fluids and/or (ii) organic matter-derived sulfur. The lack of BSR-related textures and the occurrence of organic matter in the ore are in favor of the contribution of the organically bound sulfur, though probably minimal. Based on the aforementioned discussion, it can be concluded that the source of sulfur for the ore is mainly the TSR of dissolved Triassic and Messinian sulfates, with a possible contribution from the organically-bound sulfur. Using the isotopic equilibrium equation ($\Delta^{34}S_{sphalerite-galena} = 0.73 \times 10^6/T^2$; Ohmoto and Rye, 1979), the calculated isotopic equilibrium temperature ranges between 220 and 316 °C. This temperature range is higher than the one obtained from fluid inclusion study (Th = 129–145 °C; Bejaoui, 2012). This suggests that equilibrium has not been reached (Ohmoto, 1986). This disequilibrium was likely caused by the mixing between the ascending ore-bearing hydrothermal fluids and a shallower, sulfur/sulfate-rich fluid. This mixing triggered the precipitation of sulfides and later barite at the site of deposition. The cooling of the ore-forming fluids during the fluid–rock interaction may have also contributed to the precipitation of the ore, as indicated by the occurrence of intense silicification that affected the carbonate host rocks. These ore-precipitating mechanisms are known to cause the precipitation of MVT ore deposits (e.g., Leach et al., 2006).

### 6.2. Age of ore emplacement and source(s) of metals

The absolute age of the ore emplacement has not been assigned to the Jebel Mecella and Sidi Taya ore deposits. Fieldwork, as well as sulfur isotope data led us to narrow and constrain the age of ore precipitation. Mineralization of the studied ore deposits is hosted in the Jurassic and the Upper Cretaceous rocks (Souissi et al., 1997). Hence, the ore may be post-Upper Cretaceous. However, the fact that sulfur in the barite from Sidi Taya was derived mainly from Messinian seawater imposes an upper Miocene age as the age of ore emplacement. Another line of argument in favor of an upper Miocene age is the fact that the N110 to N120°E and N160 to N170°E normal faults, formed during the Pliocene–Early Quaternary, do not host ore. Hence, the ore predated the onset of the Pliocene–Quaternary extensive tectonic phase. Based on the aforementioned arguments, the upper Miocene is the proposed age of ore emplacement in these ore deposits. The proposed age agrees with that suggested by other researchers based on geological evidence (Benchilla et al., 2003; Jemmali et al., 2011b and Souissi et al., 2013). The suggested age coincides with the second compressional upper Miocene tectonic phase that remobilized the metals for deep parts of the basin. The Pb isotopic composition of galena from Jebel Mecella and Sidi Taya are similar and overall homogenous. The Pb isotope ratios plot close to the average Pb crust evolution curve in the plumbotectonics model of Zartman and Doe (1981) (Fig. 5), suggesting a single crustal source. Overall, the Pb isotope ratios of galena from Jebel Mecella and Sidi Taya plot within the field defined by galena samples from the FZP (Souissi et al., 2013), implying similar metal source(s) of these ore deposits (Fig. 6). Owing to the radiogenic Pb signature of the analyzed galena samples, the siliciclastic Paleozoic rocks are likely a potential source of metals. Although the Paleozoic rocks are likely the main source of metals, the Triassic to Jurassic rocks, through which the deep-seated Paleozoic-derived fluids flowed, can also be a source of metals. Two interpretations can account for the overall uniformity of Pb isotopic composition in the studied ore deposits. In case the lead derived from different rock reservoirs of Paleozoic to Cretaceous age, the Pb uniformity is likely ensured through the mixing of the fluids as they traveled through the thick Paleozoic–Cretaceous rock sequences towards the loci of deposition where ore was deposited. To ensure the Pb isotopic composition's homogeneity, the mixing took place before the site of deposition. This mixing is capable of averaging and homogenizing the Pb isotopic composition of fluids prior to the site of deposition (Vaasjoki and Gulson, 1986). Alternatively, the uniformity of the Pb isotopic composition may also suggest that lead and presumably other metals derived mainly from the Paleozoic rocks, with an overall homogeneous composition.

### 6.3. Ore genesis model

Based on geology, sulfur and lead isotopes and fluid inclusion data from the literature, an ore genesis model is proposed for the Jebel Mecella and Sidi Taya ore deposits.

The N100–N120°E-trending normal faults and fractures, formed during the Cretaceous extensive phase and reactivated during the Oligocene–Miocene extensional tectonic phases, had likely acted as potential pathways for the downward fluid flow of the shallow, cooler superficial fluids into deep parts of the basin. The extensional tectonic phase, during which the superficial fluids percolated, cannot be precisely determined. Nevertheless, considering the late Miocene age of ore emplacement, this phase can be constrained to one of these extensive tectonic phases: Cretaceous, Oligocene, or early–middle Miocene. The Alpine compressional forces together with the topography gradient caused the circulation of large amounts of deep-seated fluids. The major NE–SW– and NW–SE-trending faults were reactivated during the Miocene Alpine orogeny (Morgan et al., 1998; Turki, 1985) and acted as potential pathways for the migration of the ore-forming fluids from the Paleozoic basement towards the Jurassic–Cretaceous unconformity where ore deposition occurred. At the site of deposition, the ore-forming fluids were probably mixed with a shallower, TSR-derived sulfur-rich, metal-poor fluid. This fluid mixing triggered the precipitation of sulfides at the Jurassic–Cretaceous unconformity. During the late stage, the ore-forming fluids encountered and mixed with rather $SO_4^{2-}$-rich Triassic evaporites and Messinian seawaters' reservoirs, leading to barite precipitation.

## 7. Conclusions

The geological, mineralogical observations, and the sulfur and lead isotopic geochemistry of the Jebel Mecella and Sidi Taya F–Ba–Sr (Zn–Pb) deposits provide constraints on the sources of metals and sulfur, the mode of fluids migration and ore precipitation, and the age of ore emplacement. These constraints are summarized below.

1) The ultimate source of the sulfur for barite derived from the Triassic evaporites and Messinian seawater. The sulfur of sulfides was generated by TSR process with a contribution of organically-bound sulfur.

2) The source(s) of lead and by inference other metals (Zn, Ba, Sr) is mainly the siliciclastic Paleozoic basement. The uniformity of the Pb isotope compositions of galena reflects a single homogeneous source reservoir of Paleozoic age and/or the homogenization of the Paleozoic–Cretaceous multireservoir-derived fluids in the course of their long migration to the loci of deposition.

3) The upper Miocene compressional tectonic phase had caused compression and topographic highs, which are effective for driving large amounts of the deep-seated fluids from the deep parts of the basin towards the margins.

4) At the site of deposition, the ascending metalliferous fluid encountered and mixed with cooler, metal-poor, and sulfur-rich superficial fluids. This fluid-mixing

process led to the precipitation of sulfides (galena, sphalerite) and later of sulfates (barite, celestine).

## Acknowledgments

The Tunisian Ministry of High Education and Research has granted the training for isotope analysis conducted at the Universities of Lausanne and Bern (Switzerland). We are grateful to reviewers Sophie Decrée and Thierry Olivier Bineli-Betsi for theircomments, and to Associate Editor François Chabaux for expert handling of our paper.

## References

Arfaoui, A., Soumaya, A., Ayed, N.B., Delvaux, D., Ghanmi, M., Kadri, A., Zargouni, F., 2017. Role of NS strike-slip faulting in structuring of north-eastern Tunisia; geodynamic implications. J. Afr. Earth Sci. 129, 403–416.

Bejaoui, J., 2012. Géologie, Minéralogie, Eléments en traces Inclusions Fluides, Isotopes et Modélisation génétique des Gisements à Pb–Zn et ou F, Ba de la Tunisie centro-septentrionale (Fedj Hassène,El Hamra, Ajered, El Kohol, Mecella, El Mokta et M'Tak). Thèse. Université Tunis-2, 260 p.

Benchilla, L., Guilhaumou, N., Mougin, P., Jaswal, T., Roure, F., 2003. Reconstruction of palaeo-burial history and pore fluid pressure in foothill areas: a sensitivity test in the Hammam Zriba (Tunisia) and Koh-i-Maran (Pakistan) ore deposits. Geofluids 3 (2), 103–123.

Ben Ayed, N., 1993. Evolution Tectonique de l'Avant-pays de la Chaîne Alpine de Tunisie du début du Mésozoïque à l'Actuel. Ann. Mines et Geol., Tunisie 32, 286 p.

Bouaziz, S., Barrier, E., Soussi, M., Turki, M.M., Zouari, H., 2002. Tectonic evolution of the northern African margin in Tunisia from paleostress data and sedimentary record. Tectonophysics 357 (1), 227–253.

Charef, A., 1986. La nature et le rôle des phases associées à la minéralisation Pb–Zn dans les formations carbonatées et leurs conséquences métallogéniques. Étude des inclusions fluides et des isotopes (H, C, O, S, Pb) des gisements des Malines (France), Fedj-el-Adoum et Jbel Hallouf-Sidi Bou Aouane (Tunisie). Thèse d'Etat, Nancy, France, 291 p.

Claypool, G.E., Holser, W.T., Kaplan, I.R., Sakai, H., Zak, 1980. The age curves of sulfur and oxygen isotopes in marine sulfate and their mutual interpretation. Chem. Geol. 28, 199–260.

Decrée, S., Marignac, C., De Putter, T., Deloule, E., Liégeois, J., Demaiffe, D., 2008. Pb–Zn mineralization in a Miocene regional extensional context: the case of the Sidi Driss and the Douahria ore deposits (Nefza mining district, northern Tunisia). Ore Geol. Rev. 34, 285–303.

Fallick, A.E., Ashton, J.H., Boyce, A.J., Ellam, B.M., Russell, M.J., 2001. Bacteria were responsible for the magnitude of the world-class hydrothermal base metal sulfide orebody at Navan Ireland. Econ. Geol. 96 (4), 885–890.

Jemmali, N., 2011. Le Trias du Nord de la Tunisie et les minéralisations associées: minéralogie, géochimie (traces, isotopes, O, C, S, Pb) et modèles génétiques. Thèse, Faculté des sciences de Tunis, 255 p.

Jemmali, N., Souissi, F., Vennemann, T.W., Carranza, E.J.M., 2011a. Genesis of the Jurassic carbonate-hosted Pb–Zn deposits of Jebel Ressas (North-Eastern Tunisia): evidence from mineralogy, petrography and trace metal contents and isotope (O, C, S, Pb). Geochem. Res. Geol. 61 (4), 367–383.

Jemmali, N., Souissi, F., Villa, I.M., Vennemann, T.W., 2011a. Ore genesis of Pb–Zn deposits in the Nappe zone of Northern Tunisia: constraints from Pb–S–C–O isotopic systems. Ore Geol. Rev. 40, 41–53.

Jemmali, N., Carranza, E.J.M., Zemmel, B., 2017. Isotope geochemistry of Mississippi valley type stratabound F–Ba–(Pb–Zn) ores of Hammam Zriba (province of Zaghouan, NE Tunisia). Chem. Erde-Geochem. 77 (3), 477–486.

Krouse, H.R., Viau, C.A., Eliuk, L.S., Ueda, A., Halas, S., 1988. Chemical and isotopic evidence of thermochemical sulphate reduction by light hydrocarbon gases in deep carbonate reservoirs. Nature 333, 415–419.

Leach, D., Macquar, J.C., Lagneau, V., Leventhal, J., Emsbo, P., Premo, W., 2006. Precipitation of lead–zinc ores in the Mississippi Valley-type deposit at Trèves, Cévennes region of southern France. Geofluids 6 (1), 24–44.

Machel, H., 2001. Bacterial and thermochemical sulfate reduction in diagenetic settings—old and new insights. Sediment. Geol. 140, 143–175.

Morgan, M.A., Grocott, J., Moody, R.T., 1998. The structural evolution of the Zaghouan-Ressas structural belt, northern Tunisia. Geol. Soc., Lond., Spec. Publ. 132 (1), 405–422.

Ohmoto, H., 1986. Stable isotope geochemistry of ore deposits. Rev. Mineral. Geochem. 16 (1), 491–559.

Ohmoto, H., Rye, R.O., 1979. Isotopes of sulfur and carbon. In: Branes, H.L. (Ed.), Geochemistry of Hydrothermal Ore Deposits, pp. 509–567.

Ohmoto, H., Kaiser, C.J., Geer, K.A., 1990. Systematics of sulphur isotopes in recent marine sediments and ancient sediment-hosted base metal deposits. Stable Isot. Fluid Process. Mineralization 23, 70–120.

Orr, W.L., 1974. Changes in sulfur content and isotopic ratios of sulfur during petroleum maturation, study of Big Horn basin Paleozoic oils. AAPG Bull. 58 (11), 2295–2318.

Souissi, F., 1987. Étude gîtologique et conditions de formation des gisements de fluorine (Pb–Zn-Ba) du Jebel Zaghouan (J. Stah et Sidi Taya) et du Jebel Oust, Tunisie nord-orientale. Thèse. Université Paul-Sabatier, Toulouse-3, France, 220 p.

Souissi, F., Dandurand, J.-L., Fortuné, J.-P., 1997. Thermal and chemical evolution of fluids during fluorite deposition in the Zaghouan province, north-eastern Tunisia. Miner. Deposita 32 (3), 257–270.

Souissi, F., Jemmali, N., Souissi, R., Dandurand, J.-L., 2013. REE and isotope (Sr, S, and Pb) geochemistry to constrain the genesis and timing of the F–(Ba–Pb–Zn) ores of the Zaghouan district (NE Tunisia). Ore Geol. Rev. 55, 1–12.

Southam, G., Saunders, J.A., 2005. The geomicrobiology of ore deposits. Econ. Geol. 100, 1067–1084.

Touhami, A., 1979. Contribution à l'étude géologique et métallogénique de la province fluorée tunisienne (Tunisie orientale). Rôle de l'altération dans la formation des concentrations fluorées. Thèse. Faculté des sciences de Tunis, 321 p.

Turki, M.M., 1985. Polycinématique et contrôle sédimentaire associé sur la cicatrice Zaghouan–Nebhana. Thèse d'État. Université de Tunis et Rev. Sci. Terre. CST–INRST (edit.), 7, 228 p.

Vaasjoki, M., Gulson, B.L., 1986. Carbonate-hosted base metal deposits; lead isotope data bearing on their genesis and exploration. Econ. Geol. 81, 156–172.

Zartman, R.E., Doe, B.R., 1981. Plumbotectonics — the model. Tectonophysics 75, 135–162.